FUDMA Journal of Sciences (FJS)
ISSN online: 2616-1370
ISSN print: 2645 - 2944
Vol. 10 No. 21, November, 2026, pp 200 – 204
DOI: https://doi.org/10.33003/fjs-2026-1021-5628

Brain Tumor Detection System Using Hybrid Image Segmentation Techniques

***[1]Isaac Terngu Adom, [2]Daniel Terkura Kumaga, [1]Aamo Iorliam, [3]Eke Egbigo Maryann, [1]Francis Henashima Iorawua, [4]Paul Shimlumun Amon, [1]Peter Ogbike and [5]Alex Aaron**

[1]Department of Mathematics and Computer Science, Benue State University, Nigeria, iadom@bsum.edu.ng
[2]Verbena Logic Limited, Lagos, Nigeria.
[3]Benue State University Teaching Hospital, Makurdi, Nigeria.
[4]Department of Physics, Benue State University, Makurdi, Nigeria.
[5]Department of Computer Science, Skyline University, Nigeria

*Corresponding authors' email: iadom@bsum.edu.ng

Received: 22 July 2026
Accepted: 05 Sept. 2026
Published: 02 Nov. 2026

ABSTRACT
Medical imaging plays a pivotal role in the detection and diagnosis of brain tumors, aiding clinicians in treatment planning and patient management. However, the inadequacies of using single image segmentation techniques for accurate tumor detection pose significant challenges. In this study, we propose a novel approach to enhance brain tumor detection by combining segmentation techniques from both Magnetic Resonance Imaging (MRI) and Computed Tomography (CT) scans. By leveraging the complementary strengths of MRI in soft tissue contrast and CT in bone visualization, our method aims to improve the accuracy and reliability of tumor segmentation. Through extensive experimentation and evaluation on a dataset of brain tumor images, we achieved promising results. The Dice Coefficient, a measure of segmentation accuracy, yielded a value of 0.7063, indicating substantial agreement between predicted and ground truth segmentations. Furthermore, the Intersection over Union (IoU) metric reached 0.5460, demonstrating significant overlap between segmented and true tumor regions. Additionally, our model attained a Binary Accuracy of 0.7388, reflecting high correctness in classifying tumor and non-tumor regions. The validation tests also indicate effective optimization and generalization of the segmentation model. Overall, our study underscores the potential of integrating MRI and CT scan segmentation techniques to enhance brain tumor detection accuracy, thus facilitating more precise clinical decision making and improving patient outcomes.

Keywords: Brain Tumor Detection, MRI, CT scan, Image Segmentation

INTRODUCTION

Brain tumor is an abnormal growth of cells in the brain. It also refers to a mass of tissue that grows out of control of the normal forces that regulates growth (Emekumeh et al., 2025). The symptoms of a tumor may be frequent headaches, migraines and even vision loss. Classified whether they are cancerous or not and their place of origin, tumors that are noncancerous are referred to as Benign while the cancerous tumors are Malignant. This classification is based on cellular origin and behaviour (Logeswari & Karnan, 2010; Louis et al., 2016). Despite decades of research, the precise causes of most brain tumors remain poorly understood, and only a small number of risk factors have been consistently and conclusively linked to their development (Ostrom et al., 2014). Exposure to moderate-to-high doses of ionizing radiation is the most firmly established environmental risk factor for brain and central nervous system tumors. Braganza et al. (2012), in a systematic review of eight cohort stuDices, found that elevated radiation exposure was consistently associated with increased risk of brain tumors, with the association generally stronger for meningioma than for glioma, and stronger for glioma when exposure occurred at a younger age. Vienne-Jumeau et al. (2019) similarly concluded that brain-ionizing irradiation, particularly during childhood, constitutes a well-established risk factor, noting that populations who received low-dose cranial irradiation for benign childhood conditions (such as tinea capitis) showed a substantially elevated relative risk of subsequent brain tumors. A small proportion of brain tumors, particularly gliomas, can be attributed to inherited genetic disorders, including neurofibromatosis, tuberous sclerosis, and Li-Fraumeni syndrome, though these Mendelian syndromes account for only a minority of cases (Ostrom et al., 2014). Brain tumors can present with various psychiatric symptoms, with or without neurological symptoms, an aspect that complicates the clinical picture. Patients with primary brain tumors can present with focal or generalized symptoms and/or clinical findings. At an initial stage, especially in low-grade tumors, most symptoms are focal depending on the localization of the lesion. Furthermore, generalized symptoms including headache, nausea, and vomiting develop when tumor size increases as hints for increased intracranial pressure. In addition to that, some symptoms such as headaches, visual disturbances, and epileptic seizures can also be either a focal or a generalized sign (Althe*r et al*., 2020). Once detected, the standard of care for most primary brain tumors combines maximal safe surgical resection with adjuvant radiotherapy and/or chemotherapy (Waqar et al., 2022). Medical imaging is central to the diagnostic process, with Magnetic Resonance Imaging (MRI) and Computed Tomography (CT) serving as the two most widely used modalities. MRI offers superior soft-tissue contrast and is considered the gold standard for delineating tumor boundaries, while CT is faster, more widely accessible, and better suited to detecting calcifications, hemorrhage, and bone involvement (Ghasemi et al., 2025; Ali, et al., 2025). Image segmentation is the step that isolates the suspicious tumor region from surrounding healthy tissue, and it remains one of

the most researched aspects of automated brain tumor detection (Gordillo et al., 2013). Traditional single-modality techniques include thresholding, region growing, and clustering-based methods. Sharma et al. (2023) proposed a hybrid multilevel thresholding approach for MRI segmentation that combines a Dynamic Opposite Bald Eagle Search optimization algorithm with morphological post-processing, achieving segmented outputs close to ground-truth annotations while overcoming the local-optima and slow-convergence problems of earlier metaheuristic thresholding methods. Computed Tomography scan examines patients without direct surgery but uses X-ray and a computer to produce brain images in axial fragments (Fahmi *et al*., 2020). Other brain tumor detection techniques include Positron Emission Tomography (PET) scan which detects positron-emitting radioactive tracers to visualize metabolic activity in the brain by three-dimensional mapping of administered positron-emitting radiopharmaceuticals such as F-fluorodeoxyglucose (for imaging glucose metabolism) which makes it suitable to study the body's morphological changes and biological functions (Alentorn *et al*., 2016); and the Diffusion Tensor Imaging (DTI), an MRI technique that measures the diffusion of water in brain tissue assessing the integrity of nerve pathways and identifying tumor involvement by allowing the in vivo noninvasive measurement of the translational motion of water, providing information about its anisotropy (or lack of it) in different tissues (Jelescu & Budde, 2017). From the foregoing, combining MRI and CT scans presents an efficient hybrid mechanism for detecting brain tumors while integrating the strength of both. The major contribution of this paper is the development of hybrid system for brain tumor detection using MRI and CT scans. This approach enhances the effectiveness of image segmentation in brain tumor detection.

MATERIALS AND METHODS

Dataset and Pre-processing

A novel brain tumor dataset containing 4500 2D MRI-CT slices with the original MRI and CT scans is gotten from Kaggle. Information from 41 patients were used. The pre-processing data pipeline includes pairing MRI and CT scans according to a specific time interval between CT and MRI scans of the same patient, MRI image registration to a standard template, MRI-CT image registration, intensity normalization, and extracting 2D slices from 3D volumes. The pipeline is then used to obtain classic 2D MRI-CT images from 3D Dicom format MRI and CT scans, which can be directly used as the training data for the end-to-end synthetic deep learning networks.

Pairing MRI and CT Scan

If the time interval between MRI and CT scans is too long, the information in MRI and CT images will not match. Therefore, we pair MRI and CT scans according to a certain time interval between CT and MRI scans of the same patient, which should not exceed half a year. Considering the differences both in the human brain and space coordinates of radiation images during scanning, the dataset is free from individual differences and unify the coordinates, which means all the CT and MRI images are registered to the standard template. The generated images are more accurate after registration. The registered scans have some extreme values, which introduce errors that would affect the generation accuracy. We normalize the image data and eliminated these extreme values by selecting the pixel values ranked at the top 1% and bottom 1% and replacing the original pixel values of these pixels with the pixel values of 1% and 99%. After carrying out the registration, the 3D MRI and CT scans are represented as 237×197×189 matrices. To ensure the compatibility between training models and inputs, each 3D image is sliced, and 4500 2D MRI-CT image pairs are selected as the final training data.

Algorithm of the Developed System

The algorithmic steps followed in developing the system are listed below, and the corresponding flowchart is presented in Figure 1:

Step 1: Start
Step 2: Input the dataset and preprocess it. This involves loading the MRI and CT scan data along with their corresponding labels.
Step 3: Define a custom dataset class to load and preprocess your data.
Step 4: Define data transformations using Augmentations.
Step 5: Load datasets with transformations and create data loaders for training, validation, and testing.
Step 6: Perform the training loop over multiple epochs.
Step 7: Evaluate the model on the validation and test sets.
Step 8: Display Results
Step 9: Stop

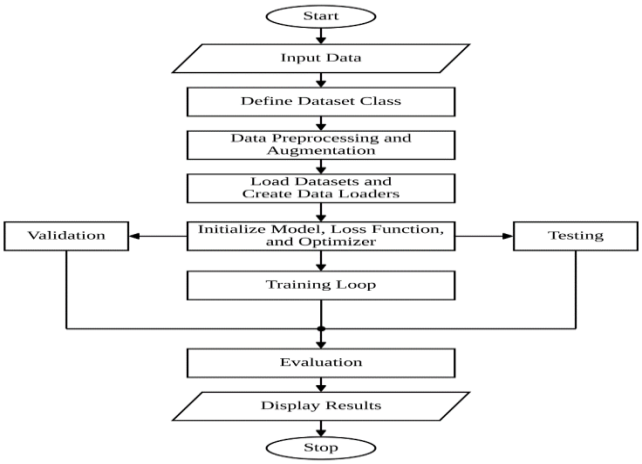


Figure 1: Flowchart Representation of the Brain Tumor Detection System

The system was built with a custom deep learning model that employs U-Net architecture commonly used for semantic segmentation tasks, particularly in medical image analysis. U-Net is known for its symmetric encoder-decoder structure

with skip connections, which helps in capturing both local and global context information while retaining spatial information.

RESULTS AND DISCUSSION

The system was tested and the results are as shown below:

Dice Coefficient

The Dice coefficient is a statistic used to gauge the similarity of two samples. In image segmentation, it measures the overlap between the predicted segmentation and the ground truth segmentation. A higher Dice coefficient indicates better overlap and therefore better segmentation accuracy. The Dice Coefficient result of 0.7063 (Figure 2) shows that there's a good overlap between the predicted segmentation and the ground truth segmentation. The Dice coefficient serves as a valuable tool for quantitatively assessing the performance of brain tumor segmentation algorithms, providing insights into the accuracy and reliability of the segmentation results, and ultimately contributing to improved clinical decision-making in the diagnosis and management of brain tumors.

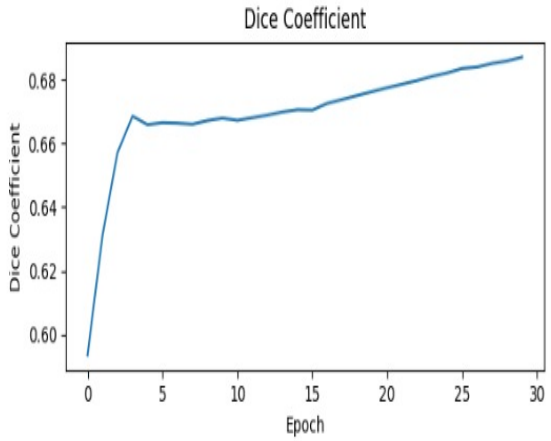


Figure 2: Dice Coefficient Result

Intersection Over Union

Intersection over Union (IoU) measures the ratio of the intersection area between the predicted segmentation and the ground truth segmentation to the union area of the two segmentations. It's another measure of segmentation accuracy, with higher values indicating better performance. The IoU result of 0.5460 shown in Figure 3 indicates that slightly more than half of the combined predicted and ground truth tumor area is shared by both segmentations.

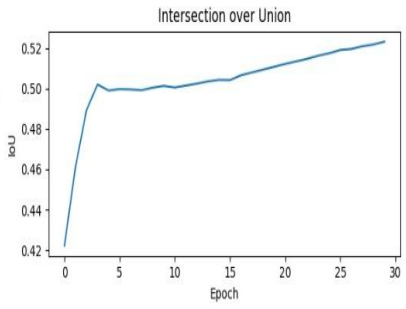


Figure 3: Intersection Over Union

Binary Accuracy

Binary Accuracy measures the ratio of correctly predicted pixels to the total number of pixels in the image. It is a measure of how accurately the model is able to classify each pixel. The Binary Accuracy result of 0.7388 (Figure 4) indicates that approximately 73.88% of pixels are being correctly classified by the model.

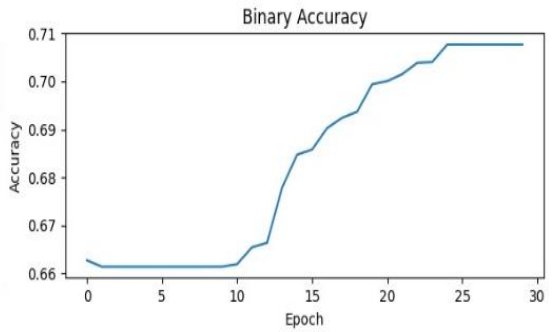


Figure 4: Binary Accuracy

Validation Loss

This metric indicates the error of the model during the validation phase of training. A lower validation loss typically suggests that the model is performing well and is generalizing properly to unseen data. The validation loss of 0.5982 and the test loss of 0.5678 are close to the final training loss of approximately 0.59 shown in Figure 5, which suggests that the model generalizes consistently to unseen data rather than overfitting the training set.

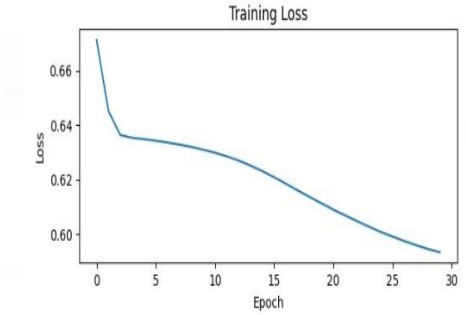


Figure 5: Validation and Test Loss (Training Loss)

Evaluation

To substantiate these findings, the system's accuracy and F-measure scores are outperformed by Emekumeh et al. (2025)'s study result. However, Emekumeh et al. (2025) assessed detection at image level, that is, whether a tumor was correctly identified in each image, whereas our study measures agreement at the pixel level, which is a stricter test of how precisely tumor boundaries are delineated. Hechri et al. (2024)'s deep learning approach reported Dice scores of 0.86, 0.81 and 0.75 for the whole tumor, tumor core and enhancing tumor respectively on the BraTS 2018 MRI dataset, and 0.85, 0.79 and 0.67 on BraTS 2019 comparison. The Dice Coefficient of 0.7063 achieved in our study falls within the range of their tumor scores and the BraTS benchmarks provide MRI sequences for patients, whereas the present model was trained on paired MRI-CT slices from 41 patients offering superior significant contribution. Studies based on CT scan do not use pixel-level segmentation, they rather carry out tumor classification. Ghasemi et al. (2025) and Ali et al. (2025) present the most recent CT scan method of classifying brain tumors while Sharma et al. (2023) used the structural similarity index rather than Dice or IoU for MRI segmentation. Our hybrid approach cannot be ranked directly with these studies as it provides an upgrade to the individual CT and MRI scans approaches. In the U-Net segmentation pipeline the overlap measures agree with each other.

CONCLUSION

The aim of this research work is to develop a Brain Tumor Detection System Using MRI and CT scan Image Segmentation Techniques. Combining the two techniques offers significant advantages over using a single modality. While MRI excels in providing detailed anatomical information and superior soft tissue contrast, CT scans offer complementary strengths such as faster acquisition times and better visualization of calcifications and bone structures. By leveraging the strengths of both modalities, clinicians can obtain a more comprehensive and accurate assessment of brain tumors, including their size, location, and characteristics. This integrated approach enhances diagnostic confidence, facilitates more precise tumor delineation, and enables better treatment planning by providing a more holistic view of the pathology. The system was built with a custom deep learning model that employs U-Net architecture commonly used for semantic segmentation tasks, particularly in medical image analysis. U-Net is known for its symmetric encoder-decoder structure with skip connections, which helps in capturing both local and global context information while

retaining spatial information. A novel brain tumor dataset containing 4500 2D MRI-CT slices was used. The original MRI and CT scans are also contained in this dataset. The model was evaluated using various evaluation metrics such as Dice Coefficient, Intersection over Union, Binary Accuracy, and Validation and Test Loss, achieving a Dice Coefficient of 0.7063, a Binary Accuracy of 0.7388 with a test loss of 0.5678. In the future, further research should be done to improve evaluation result by either using larger dataset or using extensive data augmentation. .

REFERENCES

Alentorn, A., Hoang-Xuan, K., & Mikkelsen, T. (2016). Presenting signs and symptoms in brain tumors. In *Handbook of Clinical Neurology* (Vol. 134, pp. 19–26). Elsevier. https://doi.org/10.1016/B978-0-12-802997-8.00002-5

Ali, A., Li, X., Mashwani, W. K., Abiad, M., & Tenruh, M. (2025). Computer vision based efficient segmentation and classification of multi brain tumor using computed tomography images. *Scientific Reports*, *15*, 32198. https://doi.org/10.1038/s41598-025-16825-5

Althер, B., Mylius, V., Weller, M., & Gantenbein, A. (2020). From first symptoms to diagnosis: Initial clinical presentation of primary brain tumors. *Clinical and Translational Neuroscience*, *4*(2), 2514183X2096836. https://doi.org/10.1177/2514183x20968368

Braganza, M. Z., Kitahara, C. M., Berrington de González, A., Inskip, P. D., Johnson, K. J., & Rajaraman, P. (2012). Ionizing radiation and the risk of brain and central nervous system tumors: A systematic review. *Neuro-Oncology*, *14*(11), 1316–1324. https://doi.org/10.1093/neuonc/nos208

Emekumeh, S. O., Iwedike, O. J., & Oweimieotu, A. E. (2025). Hybrid segmentation framework on brain tumor detection in medical images. *FUDMA Journal of Sciences*, *9*(8), 65-75. https://doi.org/10.33003/fjs-2025-0908-3767

Fahmi, F., Apriyulida, F., Nasution, I. K., & Sawaluddin. (2020). Automatic Detection of Brain Tumor on Computed Tomography Images for Patients in the Intensive Care Unit. *Journal of Healthcare Engineering*, *2020*. https://doi.org/10.1155/2020/2483285

Ghasemi, R., Islam, N., Bayat, S., Amin, F., Shabir, M., Rahman, S., & de la Torre Díez, I. (2025). Detection and classification of brain tumor using a hybrid learning model in CT scan images. *Scientific Reports*, *15*, 35085. https://doi.org/10.1038/s41598-025-18979-8

Gordillo, N., Montseny, E., & Sobrevilla, P. (2013). State of the art survey on MRI brain tumor segmentation. *Magnetic Resonance Imaging*, *31*(8), 1426–1438. https://doi.org/10.1016/j.mri.2013.05.002

Hechri, A., Hamed, A., & Boudaka, A. (2024). An Efficient Brain Tumor Segmentation Approach Using Cascade Convolutional Neural Networks. *International Journal of Biomedical Engineering and Technology*, 44(3).

Jelescu, I. O., & Budde, M. D. (2017). Design and Validation of Diffusion MRI Models of White Matter. Frontiers in Physics, 5, 313991. https://doi.org/10.3389/fphy.2017.00061

Logeswari, T., & Karnan, M. (2010). An enhanced implementation of brain tumor detection using segmentation based on soft computing. *2010 International Conference on Signal Acquisition and Processing, ICSAP 2010*, 243–247. https://doi.org/10.1109/ICSAP.2010.55

Louis, D. N., Perry, A., Reifenberger, G., von Deimling, A., Figarella-Branger, D., Cavenee, W. K., Ohgaki, H., Wiestler, O. D., Kleihues, P., & Ellison, D. W. (2016). The 2016 World Health Organization classification of tumors of the central nervous system: A summary. *Acta Neuropathologica*, *131*(6), 803–820. https://doi.org/10.1007/s00401-016-1545-1

Ostrom, Q. T., Bauchet, L., Davis, F. G., Deltour, I., Fisher, J. L., Langer, C. E., Pekmezci, M., Schwartzbaum, J. A., Turner, M. C., Walsh, K. M., Wrensch, M. R., & Barnholtz-Sloan, J. S. (2014). The epidemiology of glioma in adults: A "state of the science" review. *Neuro-Oncology*, *16*(7), 896–913. https://doi.org/10.1093/neuonc/nou087

Sharma, S. R., Alshathri, S., Singh, B., Kaur, M., Mostafa, R. R., & El-Shafai, W. (2023). Hybrid multilevel thresholding image segmentation approach for brain MRI. *Diagnostics*, *13*(5), 925. https://doi.org/10.3390/diagnostics13050925

Vienne-Jumeau, A., Tafani, C., & Ricard, D. (2019). Environmental risk factors of primary brain tumors: A review. *Revue Neurologique*, *175*(10), 664–678. https://doi.org/10.1016/j.neurol.2019.08.004

Waqar, M., Trifiletti, D.M., McBain, C., O'Connor, J., Coope, D.J., Akkari, L., Quinones-Hinojosa, A., & Borst, G.R. (2022). Early Therapeutic Interventions for Newly Diagnosed Glioblastoma: Rationale and Review of the Literature. *Current Oncology Reports* 24, 311–324. https://doi.org/10.1007/s11912-021-01157-0

©2026 This is an Open Access article distributed under the terms of the Creative Commons Attribution 4.0 International license viewed via https://creativecommons.org/licenses/by/4.0/ which permits unrestricted use, distribution, and reproduction in any medium, provided the original work is cited appropriately.